Autonomous quantum thermodynamic machines

Friedemann Tonner* and Günter Mahler
Institute of Theoretical Physics 1, Universität Stuttgart, D-70550 Stuttgart, Germany
(Received 8 June 2005; published 16 December 2005)

We investigate the dynamics of a quantum system consisting of a single spin coupled to an oscillator and sandwiched between two thermal baths at different temperatures. By means of an adequately designed Lindblad equation, it is shown that this device can function as a thermodynamic machine exhibiting Carnot-type cycles. For the present model, this means that when run as a heat engine, coherent motion of the oscillator is amplified. Contrary to the quantum computer, such a machine has a quantum as well as a classical limit. Away from the classical limit, it asymptotically approaches a stationary transport scenario.

DOI: 10.1103/PhysRevE.72.066118 PACS number(s): 05.70.Ln, 07.20.Pe, 03.65.Yz

I. INTRODUCTION

A classical thermodynamic machine [1] consists of a working medium (gas G) typically enclosed in a cylinder with a movable piston (mechanical degree of freedom characterized by position x). The gas G can alternatively be kept isolated or brought in thermal contact with one of two heat baths at different temperatures T_L, T_U. The coordinate x is connected with a work reservoir. Neither the work reservoir nor the various controls required to induce a cycle of isothermal and adiabatic process steps is usually modeled explicitly. For the results of the ideal Carnot efficiency to apply, the machine needs to be run in the quasistatic limit and without any friction or leakage.

Simply assuming the same conditions to apply also in the quantum limit would hardly be satisfactory: Part of the pertinent problems relate to the question of whether or not the above boundary conditions and constraints could eventually be implemented. Our quantum model should thus be a real dynamical model and as such might better be compared with its realistic classical counterparts rather than the highly idealized Carnot cycles. Unfortunately, such a detailed classical model is beyond the scope of our present investigation.

An embedded quantum system G weakly coupled to a large enough quantum environment typically relaxes into a (quasi)stationary state, which can often be characterized by thermodynamic variables like temperature T_G or entropy S_G [2,3]. This behavior is robust against perturbations; it results even if the total state is pure (total entropy $S=0$) and thus the state of the environment is far from a canonical state at any time (T does not exist).

The existence of such stationary states of G can easily be shown also as a property of phenomenological equations like master equations [4,5], then, however, assuming the preexistence of pertinent transition rates. Stationary solutions even result for specific nonequilibrium scenarios giving rise to linear transport [6]. One may thus wonder whether under autonomous conditions (i.e., no external time-dependent driving) persistent dynamical features may exist at all.

Such features, however, seem to be constitutive for quantum thermodynamic machines. They are expected to operate in a periodic fashion while being in contact with thermal environments. Unfortunately, almost all examples considered so far have been nonautonomous or, at least, semiclassical: There is a classical time-dependent external control imposed on them, which is often not even modeled explicitly.

Along these lines, a quantum version of the Otto cycle has been investigated by Kosloff *et al.* with special attention given to friction [7,8] and on the classical limit [9]. A quantum system with transitions selectively but permanently coupled to different baths and under the influence of external (time-dependent) or thermal (autonomous quantum absorption chiller) driving has been investigated with respect to cooling [10]. Work extraction from a single heat bath [11] and a so-called quantum afterburner [12] has been discussed by Scully *et al.* Bender *et al.* [13] considered basic concepts related to the quantum Carnot engine, and Lin *et al.* [14] the efficiency of a quantum heat engine. The possible impact of level crossings on maximal work extraction has been investigated by Allahverdyan *et al.* [15]. A statistical analysis of a quantum heat engine has recently been attempted by Kieu [16].

We note in passing that there is another class of models known as Brownian motors [2,17,18]. Contrary to the strictly localized machines studied here, these motors (moving in real space) are not necessarily cyclic [18]; if they are, the respective time-dependent potentials are controlled from the outside. Furthermore, the pertinent mechanical energy is basically in terms of potential rather than kinetic energy. As a result, coherence is not of major concern [19]. Heat flow is usually associated with particle flow [17], excluded in our model.

Here we will study a complete minimal quantum model capable of operating as a heat engine (or heat pump) when brought in contact with two baths of different temperature and when prepared in an initial state of a specific class. The basic model consists of a single spin ("working medium") coupled to a harmonic oscillator ("control," "work reservoir") (cf. Fig. 1). As detailed below, the respective Hamiltonian is then appropriately coupled to a split environment (two baths) and described by a phenomenological Lindblad equation. This model has a clearly defined quantum limit as well as a semiclassical and a classical limit.

We will show that due to decoherence, the machine function rapidly deteriorates close to the quantum limit: the qua-

*Electronic address: friedemann.tonner@itp1.uni-stuttgart.de

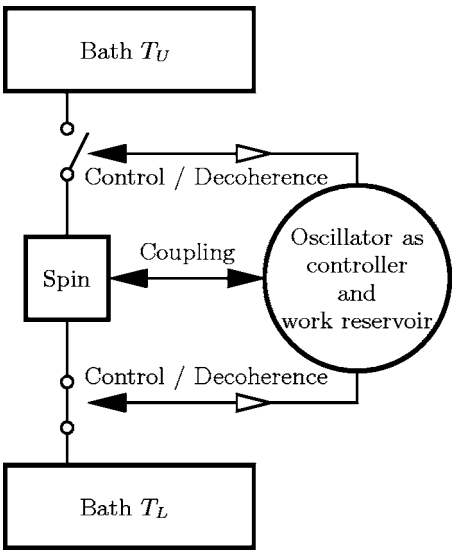

FIG. 1. System diagram of autonomous quantum thermodynamic machines.

siperiodic cycles are a transient phenomenon only on the way to a stationary transport scenario, in agreement with the above expectations.

In the classical (and semiclassical) limit, the decoherence time becomes infinite. Here we recover classical thermodynamic behavior, if in a dynamic setting.

This paper is organized as follows. In Sec. II, the pertinent Hamilton model is introduced. In Sec. III, we discuss the master equation and the implementation of time-slot operators. In Sec. IV, we supply tools to characterize the machine function (heat, work, efficiency, coherent energy), Sec. V contains the numerical results, and Sec. VI is concerned with general dynamical aspects. Our conclusions are summarized and discussed in Sec. VII. Three Appendixes give supplementary details.

II. SPIN-OSCILLATOR MODEL

A. Basic definitions

The machine M consists of a spin as the "gas" system or work medium G (which is in canonical contact with different baths at specified time slots, see below) and a control system C (harmonic oscillator).

The Hamilton operator of the total system is

$$\hat{H} = \hat{H}_{\mathrm{G}} + \hat{H}_{\mathrm{C}} + \hat{H}_{\mathrm{GC}} = \hat{H}_{\mathrm{GGC}} + \hat{H}_{\mathrm{C}} \tag{1}$$

with the local spin Hamilton operator

$$\hat{H}_{\mathrm{G}} = C_{\mathrm{G}}\hat{\sigma}_z \otimes \hat{1}, \tag{2}$$

the local harmonic oscillator Hamilton operator [20]

$$\hat{H}_{\mathrm{C}} = \hat{1} \otimes C_{\mathrm{C}}\left(\hat{b}^\dagger\hat{b} + \frac{1}{2}\right), \tag{3}$$

$$= \hat{1} \otimes \frac{C_{\mathrm{C}}}{2}(\hat{x}^2 + \hat{p}^2), \tag{4}$$

and the coupling

$$\hat{H}_{\mathrm{GC}} = C_{\mathrm{R}}\hat{\sigma}_z \otimes \hat{x} \tag{5}$$

between oscillator and spin. The (dimensionless) displacement $\hat{x}$ of the oscillator herein controls (like a piston) the mean energy splitting of the spin, where $\hat{x}=2^{-1/2}(\hat{b}^\dagger+\hat{b})$ and $\hat{p}=i\times 2^{-1/2}(\hat{b}^\dagger-\hat{b})$ are known as quadrature operators.

With the help of

$$\hat{H}_{\mathrm{GR}}(\hat{x}) = C_{\mathrm{G}}\hat{1} + C_{\mathrm{R}}\hat{x}, \tag{6}$$

we can write

$$\hat{H}_{\mathrm{GGC}} = \hat{\sigma}_z \otimes \hat{H}_{\mathrm{GR}}(\hat{x}) \tag{7}$$

and thus define an effective Hamilton operator for system G,

$$\hat{H}^{\mathrm{eff}}_{\mathrm{GGC}} = \overline{C_{\mathrm{GR}}}(\langle\hat{x}\rangle)\hat{\sigma}_z \tag{8}$$

with

$$\overline{C_{\mathrm{GR}}}(\langle\hat{x}\rangle) = \langle\hat{H}_{\mathrm{GR}}(\hat{x})\rangle = C_{\mathrm{G}} + C_{\mathrm{R}}\langle\hat{x}\rangle, \tag{9}$$

assuming $\langle\hat{\sigma}_z\otimes\hat{x}\rangle \approx \langle\hat{\sigma}_z\rangle\langle\hat{x}\rangle$ [or the dimensionless measure $\delta=\langle\hat{\sigma}_z\otimes\hat{x}\rangle/(\langle\hat{\sigma}_z\rangle\langle\hat{x}\rangle)-1\approx 0$] to be fulfilled. The effective energy splitting is then

$$\overline{\Delta E_{\mathrm{G}}}(\langle\hat{x}\rangle) = 2\overline{C_{\mathrm{GR}}}(\langle\hat{x}\rangle). \tag{10}$$

Here and in the following, the overlines indicate mean values resulting from expectation values of unsharp quantum observables. The numerical value of δ can be used as a quality measure for Eq. (10) to be a consistent concept. Typically (where the measure is not singular), δ is in the low percentage range, as long as we set $C_{\mathrm{R}}/C_{\mathrm{C}}$ to values in the same range. The validity of that effective Hamiltonian is only relevant for confirming our concepts of heat and work. Certainly we use for dynamical calculations the full Hamilton operator.

We take as initial state $\hat{\rho}(t=0)$ of the machine the product state

$$\hat{\rho}(t=0) = \hat{\rho}_{\mathrm{G}} \otimes \hat{\rho}_{\mathrm{C}} \tag{11}$$

with $\hat{\rho}_{\mathrm{G}}=\left(\begin{smallmatrix} p & 0 \\ 0 & 1-p \end{smallmatrix}\right)$ being a mixed state in $\hat{\sigma}_z$ eigenbasis. For given energy splitting ΔE_{G}, the spin may be said to be in a canonical state with temperature T_{G},

$$\frac{1-p}{p} = \exp\left(-\frac{\Delta E_{\mathrm{G}}}{T_{\mathrm{G}}}\right) \tag{12}$$

(for the isolated spin $\Delta E_G=2C_{\mathrm{G}}$). Here and in the following, all temperatures are in units of energy. (The conventional temperature would result after dividing by the Boltzmann constant k_B.) The initial oscillator state is taken to be pure,

$$\hat{\rho}_{\mathrm{C}} = |\psi_{\mathrm{C}}\rangle\langle\psi_{\mathrm{C}}|, \tag{13}$$

where $|\psi_{\mathrm{C}}\rangle=|\alpha(\phi_0)\rangle$ is a coherent state (see, e.g., [20] [excitation parameter $\alpha(\phi_0)=|\alpha|\exp(-i\phi_0)$]. For numerical rea-

sons, the state space of the oscillator will be truncated to the range $n_l, n_{l+1}, \ldots, n_{u-1}, n_u$. In the simplest case, $n_l=0$. In general, this range will reflect the initial-state distribution. This distribution controls the energy splitting of the system G but also defines the phase-locked control of the bath coupling. The Hamiltonian system thus comprises $N=2(n_u-n_l+1)$ states in total. The state (density operator $\hat{\rho}$) of machine M lives in Liouville space of dimension N^2.

Represented in the truncated Fock basis $|k\rangle$ of the oscillator, we get

$$|\alpha(\phi_0)\rangle \approx C_N \sum_{k=n_l}^{n_u} \frac{\alpha(\phi_0)^k}{\sqrt{k!}} |k\rangle \tag{14}$$

with the normalizing constant C_N. By construction we thus have an oscillatory behavior for the mean displacement of the oscillator. The effective energy splitting becomes time-dependent. We expect the splitting

$$\overline{\Delta E_{\mathrm{G}}}(\langle \hat{x} \rangle) = \overline{\Delta E_{\mathrm{G}}}(t) = 2C_{\mathrm{G}} + 2\sqrt{2} C_{\mathrm{R}} |\alpha| \cos(t + \phi_0) \tag{15}$$

for unitary dynamics and $\omega = C_{\mathrm{C}} = 1$.

The values of the constants $\{n_l, n_u, C_{\mathrm{R}}, C_{\mathrm{G}}, C_{\mathrm{C}}\}$ define the special Hamilton model of the machine M, $\{|\alpha|, \phi_0, T_{\mathrm{G}}\}$ its initial state (cf. Sec. V).

Note that—even without any bath coupling—the total system energy $E=\langle \hat{H} \rangle$ is defined here with some finite uncertainty only.

B. Thermodynamic variables for G

The instantaneous mean "effective" temperature of the spin G [cf. Eq. (12)] is

$$\overline{T_{\mathrm{G}}} = - \frac{\overline{\Delta E_{\mathrm{G}}}(\langle \hat{x} \rangle)}{\ln\left(\dfrac{\mathrm{Tr}\{\hat{P}_{11} \hat{\rho}_{\mathrm{G}}\}}{\mathrm{Tr}\{\hat{P}_{00} \hat{\rho}_{\mathrm{G}}\}} \right)} \tag{16}$$

with the reduced density operator $\hat{\rho}_{\mathrm{G}}$ of the system G and

$$\hat{P}_{kk} = |k\rangle\langle k|, \quad k = 0, 1. \tag{17}$$

Because the total system is interacting with the environment (baths), the (dimensionless) von Neumann entropy

$$S = - \mathrm{Tr}\{\hat{\rho} \ln \hat{\rho}\} \tag{18}$$

can change. We need to consider also the reduced entropy [21]

$$S_{\mathrm{G}} = - \mathrm{Tr}\{\hat{\rho}_{\mathrm{G}} \ln \hat{\rho}_{\mathrm{G}}\}, \tag{19}$$

where $\hat{\rho}_{\mathrm{G}} = \mathrm{Tr}_{\mathrm{C}}\{\hat{\rho}\}$ is the reduced density operator of G. S_{C} is defined correspondingly.

Because the total system is in a mixed state (initial preparation: canonical state in the spin system G and pure coherent state in the oscillator system C) even initially, the entropies S_{G}, S_{C} are not equal. The von Neumann entropy S_{G}, after multiplying with the Boltzmann constant k_B, can be identified with the thermodynamic entropy [initially the spin state is diagonal in its energy representation; a bath-induced transition between level 0 and 1 cannot generate coherences (off-diagonal elements in the energy representation) in system G and coherences between system G and C are not relevant for calculating the entropy of the system G]. This even holds in the dynamical case, for which the system G is not in equilibrium with the bath in contact, but with a "virtual bath" of the temperature $\overline{T_{\mathrm{G}}}$ as introduced in Eq. (16).

III. MASTER EQUATION

A. Lindblad superoperator

The dynamic evolution of a Hamilton system, weakly coupled under Markov conditions to a time-independent environment, can be represented by a Lindblad superoperator $\hat{L}$ [4,5],

$$\hat{L} = \hat{L}_{\mathrm{coh}} + \sum_m \hat{L}_{\mathrm{inc},m}, \tag{20}$$

which is constructed from a coherent part (Hamilton dynamics)

$$\hat{L}_{\mathrm{coh}} \hat{\rho} = - \frac{\mathrm{i}}{\hbar} [\hat{H}, \hat{\rho}] \tag{21}$$

and incoherent parts m

$$\hat{L}_{\mathrm{inc},m} \hat{\rho} = \hat{A}_m \hat{\rho} \hat{A}_m^\dagger - 1/2 [\hat{A}_m^\dagger \hat{A}_m, \hat{\rho}]_+. \tag{22}$$

Here the action of the environment on the considered system is described by the environment operators $\hat{A}_m$.

The open system dynamics is then given by

$$\dot{\hat{\rho}} = \hat{L} \hat{\rho} \tag{23}$$

with the formal solution

$$\hat{\rho}(t) = \exp(\hat{L}t) \hat{\rho}(0). \tag{24}$$

In our case, we want to couple the spin alternatively to two baths of different temperature during different time slots, defined by the momentary oscillator state. The bath coupling has thus to be controlled by the state of the oscillator C in an autonomous fashion (i.e., explicitly time-independent).

Under bath contact, only the occupation of the spin states should change (quasi-isothermal step), whereas the control system itself should be disturbed in the least possible way.

The environment operators are thus taken to have the following general form:

$$\hat{A}_m = \hat{A}_{\gamma_\pm^{(j)}, f^{(j)}, \pm} = \gamma_\pm^{(j)} \hat{\sigma}_\pm \otimes \hat{\Pi}^{(j)}[f^{(j)}], \tag{25}$$

with the amplitudes $\gamma_\pm^{(j)}$ (giving the direction-dependent transition rates of bath j with temperature T_j, $j=U,L$ for the upper and lower temperature, respectively), the transition operator $\hat{\sigma}_\pm$ acting on the spin subspace and a "time-slot operator" $\hat{\Pi}^{(j)}[f^{(j)}]$ acting on the oscillator subspace. The index (j) indicating bath and time slot (see Fig. 2) is dropped in the following section for clarity.

B. Time-slot operators

The idea of time-slot operators is based on the control of an incoherent process (here with respect to the spin) by test-

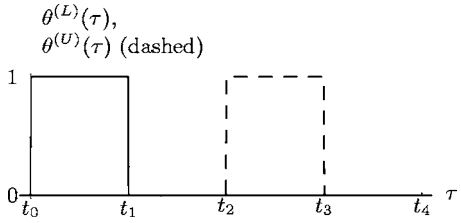

FIG. 2. Control functions $\theta^{(j)}(\tau)$ for switching on and off baths of temperature T_j $(j=U,L)$at different time slots (shown for the heat engine).

ing the momentary phase of an oscillator state. How can we generate an operator that reacts sensitively and autonomously to such a phase? To reach this goal, it is essential to have a clear picture of the behavior of an oscillator state in time. The fidelity [22]

$$F(t) = \mathrm{Tr}\{\hat{\rho}_{\mathrm{C}}(0)\hat{\rho}_{\mathrm{C}}(t)\} \tag{26}$$

is 1 at time $t=0$ and rapidly drops depending on the width of the oscillator state distribution. Equation (26) tests the time-dependent state $\hat{\rho}_{\mathrm{C}}(t)$ against its value at $t=0$. $F(t)$ is thus periodic with the oscillator frequency $\omega=C_{\mathrm{C}}$. (Three examples are discussed in Appendix A.)

We define time-slot operators as the functional

$$\hat{\Pi}[f] = \hat{\Pi}[\theta(\tau)\hat{\rho}_{\mathrm{C}}(\tau)] = N_{\Pi}\int_{\tau\in\Theta_{\omega}} \theta(\tau)\hat{\rho}_{\mathrm{C}}(\tau)d\tau \tag{27}$$

with an arbitrary scalar control function $\theta(\tau)$ defined on a single period, i.e., in the interval of length $2\pi/\omega$, e.g., $\Theta_{\omega}=[0,2\pi/\omega]$, and a (normalization) constant N_{Π}. Time is measured in units C_{C}^{-1}. The discrete Fourier transform involved (see the representation below) generates the periodicity automatically.

$$F(t) = \mathrm{Tr}\{\hat{\Pi}[\theta(\tau)\hat{\rho}_{\mathrm{C}}(\tau)]\hat{\rho}_{C}(t)\} \tag{28}$$

is a generalization of Eq. (26), which is recovered for

$$\theta(\tau) = \delta(\tau) \tag{29}$$

and $N_{\Pi}=1$.

If we choose the uniform amplitude distribution over the Fock states of the oscillator (cf. Appendix I), the definition of the time-slot operator is least state-dependent (independent of $|\alpha|$ of the actual oscillator state, there should be an overlap between the time-evolved state and the integral over states used for defining the time-slot operator),

$$|\psi_{\mathrm{C}}(t)\rangle = \frac{1}{\sqrt{n}}\sum_{k=n_l}^{n_l+n-1} e^{-i\omega kt}|k\rangle. \tag{30}$$

Then we get for $n_l=0$

$$\hat{\rho}_{\mathrm{C}}(t) = |\psi_{\mathrm{C}}(t)\rangle\langle\psi_{\mathrm{C}}(t)| = \frac{1}{n}\sum_{k=0}^{n-1}\sum_{l=0}^{n-1} e^{-i\omega(k-l)t}|k\rangle\langle l| \tag{31}$$

and thus the matrix representation of $\hat{\Pi}$ reads in the Fock basis

$$\Pi_{kl}[f] = N_{\Pi}\int_{\tau\in\Theta_{\omega}} \theta(\tau)(\rho_{\mathrm{C}})_{kl}(\tau)d\tau$$
$$= \frac{N_{\Pi}}{n}\int_{\tau\in\Theta_{\omega}} \theta(\tau)e^{-i\omega(k-l)\tau}d\tau. \tag{32}$$

This representation involves a Fourier transformation of the control function, leading us to a direct interpretation of the time-slot operator: The time-slot operator uses the basic resource of the oscillator, namely the multiples of a single frequency, to synthesize the desired control function, when the time-slot operator is applied to an evolving oscillator state.

If taken as part of an environment operator, it can therefore be used to control, for example, a state transition within another system as in Eq. (25).

Note that the environment operators act on the system all the time. The whole system is explicitly time-independent (every "time dependence" or machine function is engineered into the environment operators), in contrast with the conventional use of gates (switched on and off by external classical control) in quantum computing [22].

Thus time-slot operators are a means for incoherent state-dependent autonomous control.

The time-slot operator inherits its Hermitian property and its positivity via the definition over the density operator. It is not a projector, but a sum (integral) over projectors.

If the control oscillator is also used as a work variable (as it is in the present model) and if we do not want the time-slot operators to change the mean energy of the oscillator substantially (in order to do proper evaluation of work and heat; even then the variance of $\hat{H}$ changes), we have to further constrain the time-slot operator.

In the Lindblad time evolution, terms of the type $\hat{\Pi}|\psi_{\mathrm{C}}\rangle$ for pure initial states of the oscillator occur. We want to restrict the time-slot operator $\hat{\Pi}$ in the following sense:

$$|\langle\psi_{\mathrm{C}}\hat{\Pi}^{\dagger}|\hat{H}_{\mathrm{C}}|\hat{\Pi}\psi_{\mathrm{C}}\rangle|^2 = |\langle\psi_{\mathrm{C}}|\hat{H}_{\mathrm{C}}|\psi_{\mathrm{C}}\rangle|^2 \tag{33}$$

for any $|\psi_{\mathrm{C}}\rangle$. Thus the application of $\hat{\Pi}$ on $|\psi_{\mathrm{C}}\rangle$ will not change the mean occupation number directly, at least in an infinitesimally small time step.

This is the case if every column of the normalized Π_{kl} has the mean l,

$$\frac{1}{N_l}\sum_k k|\Pi_{kl}|^2 = l, \tag{34}$$

with

$$N_l = \sum_k |\Pi_{kl}|^2. \tag{35}$$

As the spectrum has a lower bound even for the full harmonic oscillator, this condition cannot be true for all states $|\psi_{\mathrm{C}}\rangle$ (especially for small $|\alpha|$). For a truncated oscillator, this is also a problem at the higher end of the spectrum.

But using the following cutoff procedure produces an operator that leaves the mean energy of the oscillator unchanged to "first order" in the Lindblad time evolution by

TABLE I. Process steps of heat engine.

Heat engine		Step	Start time
Compression	Isothermal T_L	1	t_0
	Adiabatic	2	t_1
Expansion	Isothermal T_U ($>T_L$)	3	t_2
	Adiabatic	4	t_3

TABLE II. Process steps of heat pump.

Heat pump		Step	Start time
Compression	Adiabatic	1	t_0
	Isothermal T_U	2	t_1
Expansion	Adiabatic	3	t_2
	Isothermal T_L ($<T_U$)	4	t_3

suppressing unbalanced time dependencies between diagonal elements of $\hat{\rho}_C$ ("second-order" effects are present via off-diagonal time dependencies). With the definition of Eq. (32), in which the absolute square of Π_{kl} is symmetric in k around $k=0$,

$$\Pi'_{kl} = \begin{cases} \Pi_{kl} & \text{if } (|k-l| \leqslant l) \wedge [|k-l| \leqslant (n-1)-l] \\ 0 & \text{otherwise.} \end{cases} \tag{36}$$

Note that this cutoff procedure for the time-slot operator destroys its Hermitian property, nevertheless the control function is not compromised severely.

As the bath coupling in Lindblad form is phenomenological, we have to put all its properties into the control function $\theta(\tau)$. Thus it should depend in our context on the parameters $\overline{\Delta E_G}$, T and the transition direction.

If the coupling strength to the bath was large, the bath could "see," in principle, the dynamics and changes in the spectrum of the system (time scale of the system larger than that of the bath). If the coupling was weak, the bath should see only an average spectrum (but it always has to see the time-dependent phase of the oscillator). So the control function can be, as an example, a sine times a rectangular function (sinusoidal energy splitting) or a rectangular function only.

IV. CARNOT MACHINE CYCLES

A. Choice of amplitudes $\gamma_{\pm}^{(j)}$ and control functions $\theta^{(j)}(\tau)$

The general characteristics of the time-slot operators acting on system C combined with transition operators in the system G do not yet completely define the system characteristics. The number and form of the control functions have to be specified.

The simplest way to define a thermodynamic machine in the quantum regime is to mimic a classical thermodynamic machine. Such a machine undergoes several steps (strokes) such that the properties of the working medium G do not change over one complete cycle. Cycles are then repeated at will. Because we alternatively use canonical contacts to the baths and isolation from baths (steered by the control function), the analogous system is the Carnot machine [1]. A Carnot machine is a four-stroke machine, which can run in two directions, as a heat pump and a heat engine, respectively, depending on the order in time of isothermal/adiabatic expansion/compression process steps.

The process steps are summarized in Tables I and II. Step 4 ends with time t_4, which is then identified with time t_0 of the next cycle.

As our model is autonomous, we have to precalculate the time-independent environment operators $\hat{A}_i$ from an assumed (virtual) time evolution of the oscillator, which is taken to be unitary. Note that as the environment operators exhibit back-action on the oscillator, the real time evolution is not unitary.

One simple way to define the control function on the time interval $\Theta_\omega=[t_0=0, t_4=2\pi/\omega]$ is to use the normalized rectangular function $\theta(\tau)=\mathrm{rect}(\tau;\tau_a,\tau_b)\equiv H(\tau-\tau_a)-H(\tau-\tau_b)$, where $H(\tau)$ is the Heaviside step function and τ_a and τ_b are constants $\tau_a<\tau_b$. This means for a machine in contact with the bath T_j $(j=U,L)$: $\theta^{(j)}(\tau)=\mathrm{rect}(\tau;\tau_a^{(j)},\tau_b^{(j)})$ with the constants for the heat engine: $\tau_a^{(L)}=t_0$, $\tau_b^{(L)}=t_1$, $\tau_a^{(U)}=t_2$, $\tau_b^{(U)}=t_3$ (cf. Fig. 2) and for the heat pump: $\tau_a^{(U)}=t_1$, $\tau_b^{(U)}=t_2$, $\tau_a^{(L)}=t_3$, $\tau_b^{(L)}=t_4$.

We calculate the time-slot operators $\hat{\Pi}^{(j)}[\theta^{(j)}(\tau)\hat{\rho}_C(\tau)]$ for each bath $j=U,L$ from these requirements [cf. Eq. (27)], apply the cutoff procedure [cf. Eq. (36)], and normalize them $[N_\Pi^{(j)}=1/F^{(j)}(\tau_N^{(j)})]$ with respect to the fidelity of Eq. (28) at time $\tau_N^{(j)}=(\tau_a^{(j)}+\tau_b^{(j)})/2$. The typical behavior of the fidelities of the resulting operators $\hat{\Pi}'$ is depicted in Fig. 3. They can be viewed as a finite realization of the control functions (cf. Fig. 2).

We time-average the energy splitting of Eq. (15) over the respective time slot

$$\widetilde{\Delta E_G}^{(j)} = \frac{1}{\tau_b^{(j)}-\tau_a^{(j)}} \int_{\tau_a^{(j)}}^{\tau_b^{(j)}} \overline{\Delta E_G}(\tau)\, d\tau \tag{37}$$

and calculate the corresponding occupation numbers [cf. Eq. (12)] from

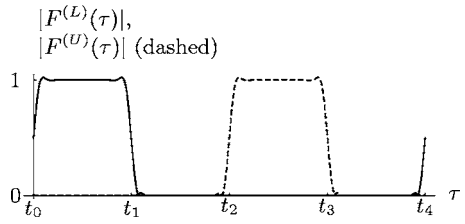

FIG. 3. Modulus of the fidelities $F^{(j)}(\tau)$, Eq. (28), resulting from the respective control functions $\theta^{(j)}(\tau)$, $j=U,L$, as shown in Fig. 2. Here we have used the cutoff version $\hat{\Pi}'$ according to Eq. (36) for the heat engine M_1 (see Sec. V). The imaginary parts of $F^{(j)}(\tau)$ are typically two orders smaller than the respective real parts. The finite slope stems from the finite width of the oscillator state occupation number distribution.

$$\frac{1-p^{(j)}}{p^{(j)}} = \exp\left(-\frac{\widetilde{\Delta E_{\mathrm{G}}}^{(j)}}{T_j}\right) \tag{38}$$

to define the amplitudes of the environment operators of Eq. (25),

$$\gamma_-^{(j)} = C_{\mathrm{B}}\sqrt{p^{(j)}}, \quad \gamma_+^{(j)} = C_{\mathrm{B}}\sqrt{1-p^{(j)}}, \tag{39}$$

where C_{B} is a global amplitude factor used for adjusting the total bath strength. This approach assumes that the baths only see the mean splitting during a time slot.

Another way to calculate the amplitudes would be to calculate the instantaneous rates (splitting changes with time continuously, so do the rates) and to use them as control function.

B. Heat and work

For a two-level system, restricted to states diagonal in its energy representation and subject to external control of its spectrum, $E_k = E_k(x)$ [cf. Eq. (10)], the Gibbsian fundamental form

$$d\bar{E} = TdS + dW \tag{40}$$

always applies, where $dW = \xi dx$ is the work, ξ is an intensive parameter, and x is an extensive work variable as $\langle \hat{x} \rangle$ in our spin-oscillator model. $dQ = TdS$ is the heat. In order to show this, consider the mean internal energy

$$\bar{E} = \sum_k w_k E_k, \tag{41}$$

$$\Rightarrow d\bar{E} = \sum_k dw_k E_k + \sum_k w_k dE_k. \tag{42}$$

According to our assumptions, we have

$$dE_k = \frac{\partial E_k}{\partial x} dx, \tag{43}$$

$$d\bar{E} = \sum_k dw_k E_k + \underbrace{\sum_k w_k \frac{\partial E_k}{\partial x}}_{\xi} dx = \sum_k dw_k E_k + dW. \tag{44}$$

On the other hand, the entropy is given by

$$S = -\sum_k w_k \ln w_k \tag{45}$$

so that

$$dS = -\sum_k dw_k \ln w_k - \sum_k w_k d(\ln w_k). \tag{46}$$

Observing

$$d \ln w_k = \frac{1}{w_k} dw_k, \quad \sum_k dw_k = 0, \tag{47}$$

the second term in Eq. (46) is zero.

If the state is canonical with $w_k = (1/Z)e^{-\beta E_k}$ (for a two-level system restricted to states diagonal in energy representation, this form always applies),

$$\ln w_k = -\beta E_k - \ln Z, \tag{48}$$

$$\Rightarrow dS = \beta \sum_k dw_k E_k, \quad \beta = \frac{1}{T}, \tag{49}$$

and Eq. (44) becomes Eq. (40), as claimed.

In general, heat and work are not state functions, only their sum, the total internal energy. So, how can these parts be measured or calculated? For a machine cycle we have $\Delta\bar{E} = 0$, and thus we conclude from Eq. (40) that $dW = -TdS$. This means that per cycle

$$\Delta W = -\oint TdS. \tag{50}$$

As usual, the exchanged work per cycle can be obtained from the area in $T(S)$ space. In the present case, T will be an effective temperature, which is not necessarily fixed by the external heat baths.

C. Energy balance

For the present (autonomous) model, heat and work can alternatively be identified with the change of the total energy for specific steps.

The heat flowing into the spin-oscillator system M can be monitored by looking at the difference of $\langle \hat{H} \rangle$ at the time of the beginning of the respective isothermal process step and at its end. Consider, e.g., for the heat engine (cf. Table I)

$$\overline{\Delta E_{32}} = \langle \hat{H}(t_3) \rangle - \langle \hat{H}(t_2) \rangle. \tag{51}$$

$\overline{\Delta E_{32}} = \overline{\Delta Q_U}$ is the heat per cycle flowing from the bath with temperature T_U ($> T_L$) into the system G.

The energy gained per cycle remains in the total system (cf. Table I),

TABLE III. Machine parameters.

	C_{C}	C_{G}	C_{R}	C_{B}		ϕ_0
All machines	1	5	$0.05\times\sqrt{2}$	0.8		π
	n_l	n_u	$\lvert\alpha\rvert$	T_L	T_U	$\overline{T_{\mathrm{G}}}$
Heat engine M_1	91	168	$0.8\times\sqrt{200}\approx 11.31$	1	5	2.935
Heat pump M_2	0	58	6	5	5.1	4.596
Heat engine M_3	6	29	$0.8\times\sqrt{30}\approx 4.38$	5	20	10.445

$$\overline{\Delta E_{40}} = \langle \hat{H}(t_4) \rangle - \langle \hat{H}(t_0) \rangle. \tag{52}$$

The system G is quasicyclic, so the work must completely be stored in the system C (oscillator, functioning as a work reservoir). As confirmed numerically, this energy gain, $\overline{\Delta E_{40}}$, coincides (within tight limits) with the work $|\overline{\Delta W}|$ according to expression (50).

Finally, the efficiency for the heat engine reads, as in the classical case [1],

$$\bar{\eta} = \frac{|\overline{\Delta W}|}{\overline{\Delta Q_U}}. \tag{53}$$

Note that $\overline{\Delta W}$ and $\overline{\Delta Q_U}$ are averaged values (expectation values). In the quantum limit, fluctuations (nonzero variances) will become sizable.

The analysis of the heat pump can be carried out correspondingly.

D. Storage of work

Contrary to the classical case $\overline{\Delta E_{40}}$ is not fully associated with coherent motion (increase of oscillator amplitude). For a small excitation $|\alpha|$, the oscillator feels the effect of a finite coupling constant C_R on the eigensystem and the decoherent backaction of the time-slot operators. These effects diminish the amount of coherently stored work and will be dealt with under the general term "decoherence." In this sense the storage is not completely "mechanical."

As the manipulation of the system G is accomplished by a coupling to displacement $\hat{x}$ of the oscillator C with the matrix representation (Fock basis states $|k\rangle$)

$$x_{kl} = 2^{-1/2}(\sqrt{k}\,\delta_{k,l+1} + \sqrt{k+1}\,\delta_{k+1,l}), \tag{54}$$

the energy coherently stored in the oscillator could be defined as the energy the oscillator would have in a coherent state with the same matrix elements in the first off-diagonal. A direct construction of such an analogous state is given in Appendix B.

Here we are only interested in analyzing the distribution of the first off-diagonal elements of the reduced density matrix of the system C.

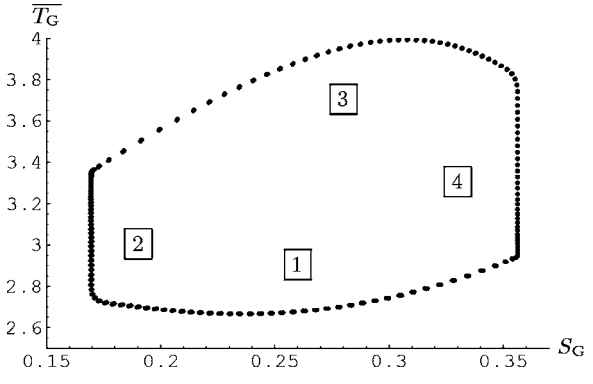

FIG. 4. Autonomous quantum heat engine M_1: Temperature $\overline{T_G}$ and entropy S_G (four cycles superimposed; each of the four steps marked by boxed numbers). $\overline{T_G}$ is given in units of C_C [Eq. (3)], S_G is dimensionless.

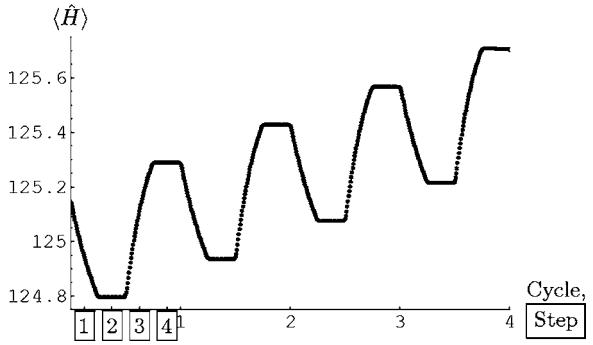

FIG. 5. Autonomous quantum heat engine M_1: Average total system energy $\langle \hat{H} \rangle$ over four machine cycles. Process steps are numbered (cf. Fig. 4). Energy in units of C_C.

As the first off-diagonal does not have to be normalized (contrary to the diagonal), we first calculate the norm (zeroth raw moment)

$$N_0 = \sum_{k=n_l}^{n_u-1} |\rho_{k,k+1}|. \tag{55}$$

The distribution function $f(k+1) = (1/N_0)|\rho_{k,k+1}|$ can then be analyzed in terms of its moments, the mean (first raw moment)

$$\mu = \sum_{k'=n_l+1}^{n_u} k' f(k'), \tag{56}$$

and its variance (second central moment)

$$\sigma^2 = \sum_{k'=n_l+1}^{n_u} (k'-\mu)^2 f(k'). \tag{57}$$

The resultant behavior of $\langle \hat{x} \rangle$ at times where the first off-diagonal is real can be expressed in good approximation by these three moments,

$$|\langle \hat{x} \rangle| \approx \sqrt{2} N_0 \left(-\frac{\sigma^2}{8\mu^{3/2}} + \sqrt{\mu} \right). \tag{58}$$

In the general case of a heat engine $|\langle \hat{x} \rangle|$ has a local maximum, which can be chosen to lie at positive times by adjust-

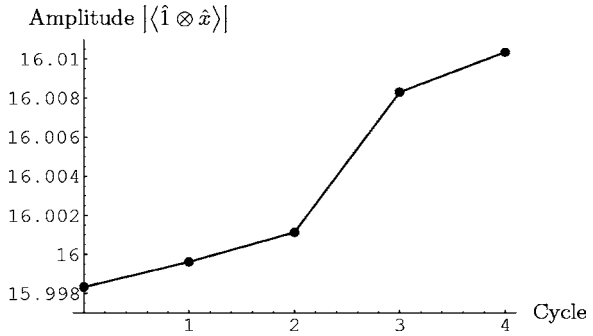

FIG. 6. Autonomous quantum heat engine M_1: Dimensionless amplitude of oscillator C over four machine cycles. Note the coherence amplification for these parameters of the heat engine.

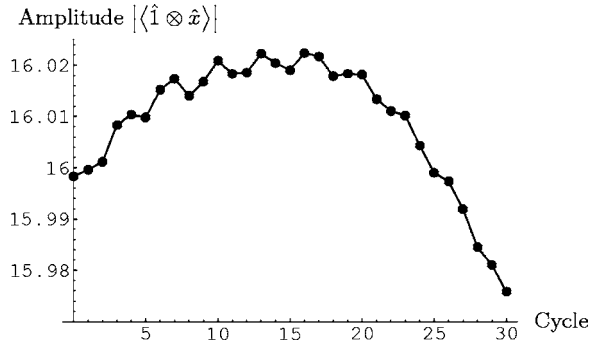

FIG. 7. Same as Fig. 6, but over 30 machine cycles. Finally decoherence is stronger, and the initial coherence amplification vanishes.

ing the parameters that influence the moments. So the oscillator amplitude typically rises until the decoherence effects take over.

V. NUMERICAL RESULTS

As we want to maximize the effect of the bath on the spin while minimizing the decoherence on the oscillator, we choose the bath action to be approximately on the same time scale as the oscillator. Furthermore, the mean energy splitting of the spin has to be large in relation to the oscillator energy C_C to fulfill the weak-coupling condition to both the oscillator and the bath.

We will consider three sets of parameters (see Table III). The heat engine results (machine M_1) are presented in Figs. 4–10. The heat pump M_2 results are shown in Figs. 11–14 and 18. The heat engine M_3 helps to demonstrate decoherence effects in Figs. 15–17.

The operators $\hat{A}_{\gamma_+^{(U)},f^{(U)},+}$ and $\hat{A}_{\gamma_+^{(L)},f^{(L)},+}$ (and likewise $\hat{A}_{\gamma_-^{(U)},f^{(U)},-}$ and $\hat{A}_{\gamma_-^{(L)},f^{(L)},-}$) have zero overlap only approximately, but they are traceless.

The Lindblad superoperator $\hat{L}$ is represented as an $N^4 = 2^4(n_u - n_l + 1)^4$-dimensional matrix. Sparsity of the matrix is made use of (only nonzero elements are being held in memory).

To save computational time for large systems (especially machine M_1), the harmonic oscillator is simulated in a state space truncated below a certain occupation number (if the occupation number in the initial state is smaller than 0.25% of the maximum occupation number, for machine M_1 and M_3). In this truncated space, the cutoff procedure for the time-slot operators, Eq. (36), has always been applied.

The time evolution is calculated by the free software package EXPOKIT [23], which calculates ρ for some time steps t.

The stationary state is calculated using the SPOOLES library [24] and the ARPACK package [25].

Figure 4 shows the quasicyclic behavior of the heat engine M_1. For the ideal Carnot engine, this closed trajectory in T_G/S_G space would be rectangular; we see that the parts 1 and 3 deviate from isotherms. Tuning the parameters of the machine toward the more quasistatic regime (large C_B^2 against ω), we would expect a closer resemblance to isotherms. The ideal Carnot efficiency would be $\eta_{\text{Carnot}} = 1 - T_L/T_U = 0.8$. Here we find $\bar{\eta} = 0.29$, mainly due to dynamical effects. Reductions of the same order are well known also for classical (dissipative) models [26].

Figure 5 shows the total system energy $\langle \hat{H} \rangle$: Note that our machine is freely running, so the mechanical energy piles up in the oscillator (cf. also Fig. 6). Alternatively, the change in system energy per cycle can be calculated from the $S_G T_G$ diagram [cf. Eq. (50)] with deviations of approximately 1% per cycle for machine M_1 (stemming from the residual direct action of the time-slot operators). The increase of the oscillator amplitude $\langle \hat{x} \rangle$ is finally reversed due to decoherence

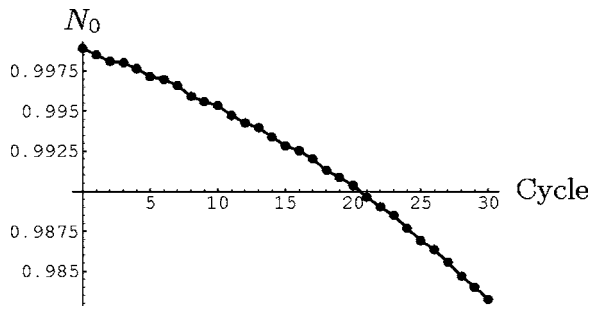

FIG. 8. Moment analysis of $|\langle \hat{x} \rangle|$ for autonomous quantum heat engine M_1: normalization factor N_0 of the first off-diagonal (real part) of $\hat{\rho}_C$ over the cycle number (see text).

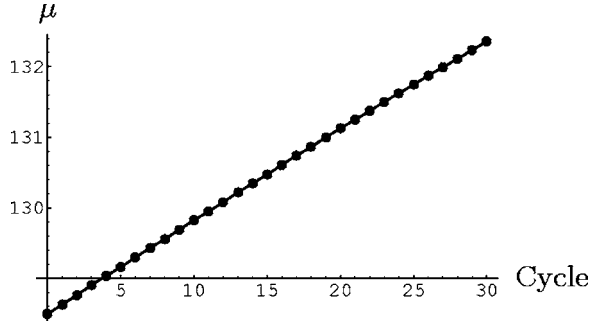

FIG. 9. Moment analysis of $|\langle \hat{x} \rangle|$ for autonomous quantum heat engine M_1: mean μ of the first off-diagonal (real part) of $\hat{\rho}_C$ over the cycle number (see text).

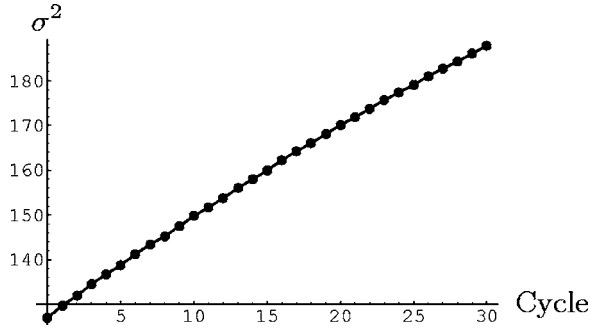

FIG. 10. Moment analysis of $|\langle \hat{x} \rangle|$ for autonomous quantum heat engine M_1: variance σ^2 of the first off-diagonal (real part) of $\hat{\rho}_C$ over the cycle number (see text).

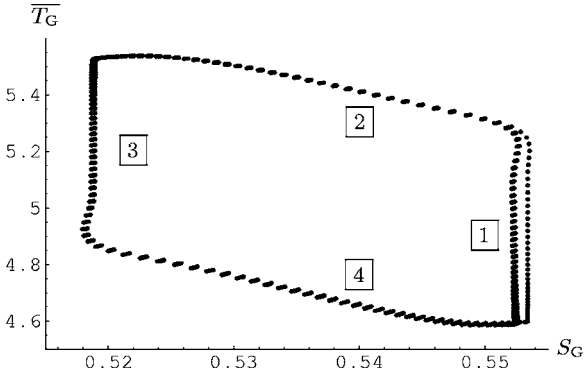

FIG. 11. Autonomous quantum heat pump M_2: Temperature $\overline{T_G}$ in units of C_C and entropy S_G (four cycles superimposed; each of the four steps marked by boxed numbers).

(Fig. 7). Certainly, the exact onset of the reversal and the degree of coherence amplification is dependent on numerical details, as, e.g., the state cutoffs n_l and n_u: Near the border of the artificially cut off spectrum of the oscillator, the eigensystem is changed. The behavior of $\langle\hat{x}\rangle$ is analyzed according to Eq. (58) in Figs. 8, 9, and 10: The norm N_0 [Eq. (55)] drops with increasing time, which accounts for the decoherence induced by the time-slot operators and by the transition operators $\hat{\sigma}_\pm$ via the coupling (C_R). The mean μ [Eq. (56)] rises almost linearly with time—this corresponds to the picture of coherent energy transfer from the system G to the system C (and the increase of the mean total energy in C). The variance σ^2 [Eq. (57)] rises approximately linearly in time, too. This is reminiscent of a random-walk dynamics induced by the action of the time-slot operators.

In order to check the consistency of our model, we performed an additional run of the machine M_1, but with $T_U = T_L = 1$. As expected, the residual energy change of the total system after four cycles is then negligible (reversed sign and more than two orders lower) and the amplitude $\langle\hat{x}\rangle$ decreases. The small residual energy change can be attributed to the direct action of the time-slot operators and/or the energy splitting averaging method used for the generation of the time-slot operators.

The quasicyclic behavior of the heat pump M_2 is summarized in Fig. 11. Again, the trajectories deviate from the ideal rectangular form of an ideal Carnot engine. Figure 12 shows

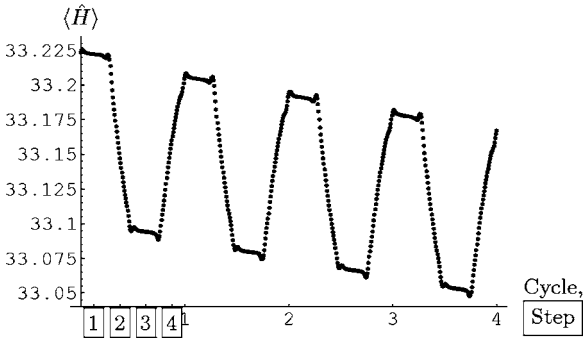

FIG. 12. Autonomous quantum heat pump M_2: Average total system energy $\langle\hat{H}\rangle$ in units of C_C over four machine cycles. Process steps are numbered (cf. Fig. 4).

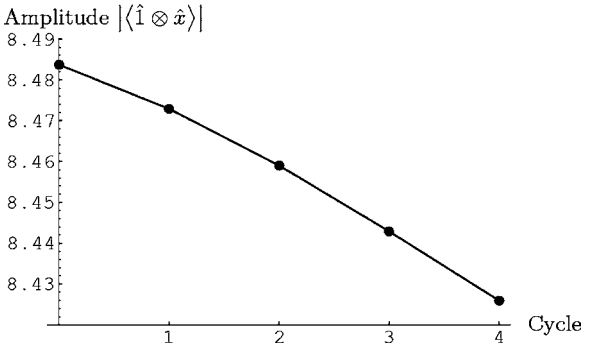

FIG. 13. Autonomous quantum heat pump M_2: Dimensionless amplitude of oscillator C over four machine cycles. The amplitude decreases as coherently stored work is used to pump heat from the cold to the hot reservoir.

the total system energy $\langle\hat{H}\rangle$. Note that the change in system energy during the adiabatic phases stems from the residual direct action of the time-slot operators. The decrease of the oscillator amplitude $\langle x\rangle$ is given in Fig. 13.

VI. LIMITING BEHAVIOR

A. Short-time and intermediate time behavior

The total system is prepared in a mixed state for system G and a pure state for the system C. Normally, the state of the system G is not a quasicyclic state [for example, if we choose quasistatic equilibrium states (isothermal contact with either bath $j=U$ or $j=L$), but drive dynamically, which we always do, our machine remains a dynamical machine unless $\omega\to 0$]. System G will therefore show an initial adaptive dynamics, until it relaxes to a quasicyclic state, as long as the state space of C is large enough (see Fig. 14).

System C performs a decohering dynamics (see, for example, machine M_3 in Figs. 15, 16, and 17). It gains steadily in entropy and takes up energy from the baths via the system G (or the other way around for different running direction, heat pump). Only the bath transitions transfer energy to and from the oscillator C via its coupling to system G, because the coupling does not change the eigenstate system of G.

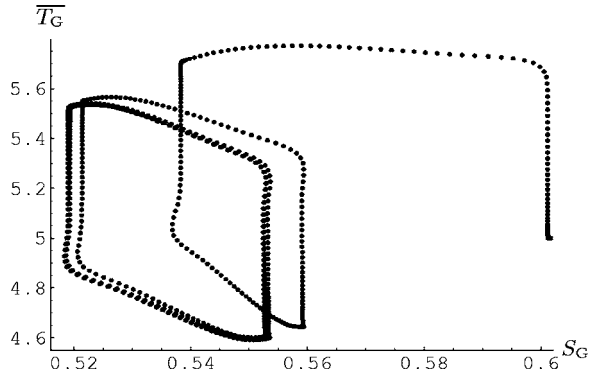

FIG. 14. Autonomous quantum heat pump M_2: Initial adaptive dynamics in the plane of temperature $\overline{T_G}$ and entropy S_G for eight cycles until a quasicyclic state for G is established.

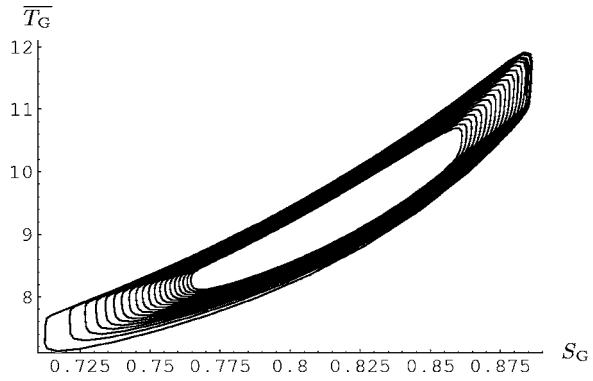

FIG. 15. Autonomous quantum heat engine M_3: Temperature $\overline{T_G}$ in units of C_C and entropy S_G (20 cycles superimposed). Spiraling in this plot is the effect of decoherence on the oscillator.

However, the amplitude $\langle x \rangle$ indicating the coherent mechanical energy decreases (Fig. 17).

B. Long-time limit

The stationary state and thus the long-time behavior can be extracted from the eigenstate corresponding to the eigenvalue 0 of the Lindblad operator $\hat{L}$. All other eigenvalues are complex with negative real part, so they will die away in time.

Qualitatively, the stationary state represents energy transport through the machine induced by the external temperature difference (cf. [27,28]). The stationary state is approximately diagonal in the oscillator subspace (mean total off-diagonal element strength for heat pump M_2 in ρ: 1.83×10^{-6}), but depends on the original running direction of the machine. The asymptotic state for the spin is thermal with a temperature between those of the two baths ($\overline{T_G} = 5.056$ for heat pump M_2). The oscillator is in a nonthermal state: The heat engine produces a state with maximal occupation at some higher energy, with approximately a power-law decay in occupation number to lower levels. In the case of the heat pump, the steady state of the oscillator is a low-energy state (cf. Fig. 18), with high occupation at the lowest level and approximately power-law decay to higher energies.

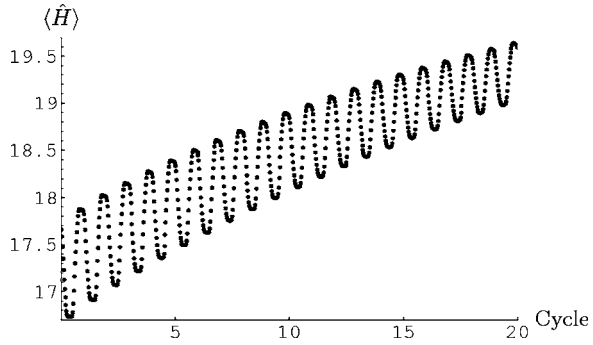

FIG. 16. Autonomous quantum heat engine M_3: Average total system energy $\langle \hat{H} \rangle$ in units of C_C over 20 machine cycles. Note that even with severe decoherence there is machine function left (increase in not coherently stored energy).

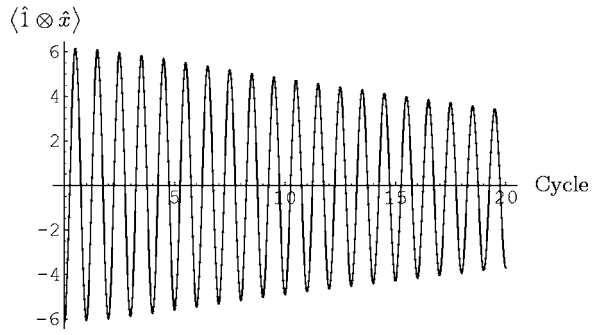

FIG. 17. Autonomous quantum heat engine M_3: Dimensionless displacement $\langle \hat{x} \rangle$ of oscillator C over 20 machine cycles. The coherently stored energy decreases.

The increase of $(\rho_C)_{kk}$ at the high-energy side seen in Fig. 18 is an artifact of the respective state truncation.

C. Quantum limit and classical limit

It is remarkable that this model is scalable, to both the quantum and the classical limit. The quantum limit is achieved for a single-spin system (the least possible) and $|\alpha| \approx 1$. As the control system is then roughly of the same dimension as the system to control, any machine function tends to vanish in this limit.

The classical limit corresponds to the ordinary thermodynamic machine, in which the control is classical (no backaction on the control system) and the work remains coherent ("mechanical," no deterioration of work needs to be regarded). The full classical limit requires us to increase the number of spins n_ν (qualitatively simulating the spectrum of a many-body system as an approach to a classical work medium),

$$\hat{H}_G = C_G \sum_{\nu=1}^{n_\nu} \hat{\sigma}_z(\nu), \tag{59}$$

$$\hat{H}_{GC} = C_R \sum_{\nu=1}^{n_\nu} \hat{\sigma}_z(\nu) \otimes \hat{x}. \tag{60}$$

The environment operators are generalized accordingly,

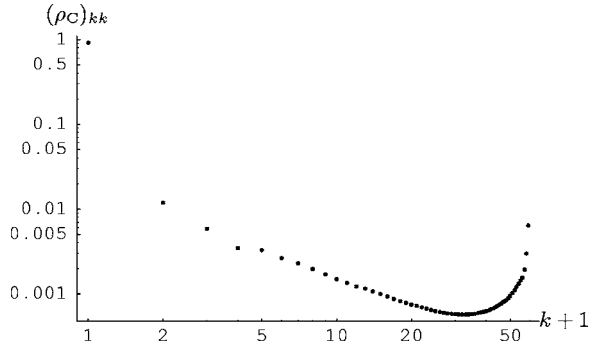

FIG. 18. Autonomous quantum heat pump M_2: Diagonal elements in Fock representation of the reduced density operator $\hat{\rho}_C$ of the stationary state.

$$\hat{A}_{\gamma_{\pm}^{(j)},f^{(j)},\pm} = \gamma_{\pm}^{(j)} \sum_{\nu=1}^{n_\nu} \hat{\sigma}_{\pm}(\nu) \otimes \hat{\Pi}^{(j)}[f^{(j)}]. \tag{61}$$

Coupling and transition operators are thus replaced by their collective counterparts of the spin network. The classical limit is achieved as $n_\nu \to \infty$ and $|\alpha| \to \infty$. As $|\alpha|$ increases, C_R must decrease to keep the coupling energy constant. So it is easily seen that the eigensystem of the harmonic oscillator becomes part of the eigensystem of the total system in the classical limit. The suppression of backaction of the $\hat{\Pi}$ operators on the oscillator has to be considered separately (see Appendix III). Only for finite values of $|\alpha|^2$ do we get decoherence. Thus in the classical limit the evolution of the harmonic-oscillator system under the operator $\hat{\Pi}$ in the incoherent Lindblad operator is, indeed, a purely coherent one.

The function $F^2(t)$ according to Eqs. (28) and (29) can be viewed as sampling the control function $\theta(\tau)$ more and more accurately as it becomes sharper (see Appendix C). In the classical limit $\theta(\tau)$ is sampled exactly, and classical parametric control is recovered.

VII. CONCLUSIONS AND DISCUSSION

To the best of our knowledge, this is the first investigation of autonomous quantum thermodynamic machines.

We have proposed a system theoretical model in the context of the Lindblad approach (open system). Its functionality is a property of the embedding (interface), not of the system as such.

The influence of the environment (two split baths) has been modeled via so called time slot operators, which use the excitation spectrum of the oscillator to control another system (the spin) by means of an arbitrary control function, even near the quantum limit. This is a special form of a quantum control encoded into the system design.

In our model, heat occurs in the gas system (the spin), mechanical energy ("work") in the control system (oscillator). Mechanical energy is of two kinds: Coherent (at the start and partially while running) and incoherent (only on the diagonal of the density matrix), while in the classical case all mechanical energy would be stored coherently. Even for small control systems and a single spin as the gas system, an increase in the coherent energy from this decoherent dynamics is possible.

We have proposed ways of analyzing coherent work and to differentiate it from decoherent work (moment analysis and analogous coherent state construction).

The gas subsystem (the spin) has been shown to behave like a classical system would if driven dynamically. The machine efficiency is therefore definable as in the classical case; it is smaller than the Carnot efficiency.

Because of the dynamical model used here, the momentary temperatures in the system deviate from the quasistatic temperatures one would expect for a strict Carnot cycle (this is not a quantum effect; it would likewise be found in the classical thermodynamic machine outside the quasistatic regime). The machine operates in an irreversible way.

After settling to a quasiperiodic equilibrium (time scale of the gas system), the system shows machine function before finally reaching (time scale of the decoherence of the control system) its stationary state. The stationary state depends on the running direction of the machine. In any case it corresponds to energy transfer between the two baths ("leakage").

In the intermediate time regime, time-scale separation holds, and over a finite range in time, machine function can be observed. Even a coherent increase of energy is observable (on a smaller time scale than the machine function itself).

Here the control system C is used also to store the (mechanical) energy to pump the heat, or the energy gained under heat engine operation. It has thus informational (control) and energetic properties. In fact, C has three functions: an effective "piston," control of bath couplings, and work reservoir.

Contrary to quantum gates, our machine has a quantum limit and a classical limit.

In the quantum limit (number of spins $n_\nu = 1$, coherent excitation of the oscillator $|\alpha| \approx 1$), the backaction of the control on the control system is substantial and leads to decoherence.

In the classical limit (number of spins $n_\nu \to \infty$, $|\alpha| \to \infty$), classical control (no back-action, fully coherent energy of the oscillator) is recovered.

ACKNOWLEDGMENTS

We thank M. Hartmann, M. Henrich, Ch. Kostoglou, M. Michel, H. Schmidt, and M. Stollsteimer for fruitful discussions. This work has been supported by the Landesstiftung Baden-Württemberg.

APPENDIX A

1. Overlap between coherent states

If the state $|\psi_C\rangle$ of a harmonic oscillator is prepared in a coherent state (Glauber state)

$$|\alpha(t=0)\rangle = e^{-|\alpha|^2/2} \sum_{k=0}^{\infty} \frac{\alpha^k}{\sqrt{k!}} |k\rangle \tag{A1}$$

and if

$$\hat{U}(t) = \sum_{k=0}^{\infty} e^{-iE_k t} |k\rangle\langle k| = \sum_{k=0}^{\infty} e^{-i\omega k t} |k\rangle\langle k|, \tag{A2}$$

where $\omega = C_C$ denotes the oscillator frequency and E_k its eigenenergies (the nonobservable global phase stemming from zero point energy has been neglected), we get for the unitary time evolution (t in units C_C^{-1})

$$|\alpha(t)\rangle = \hat{U}(t)|\alpha(0)\rangle = e^{-|\alpha|^2/2} \sum_{k=0}^{\infty} e^{-i\omega k t} \frac{\alpha^k}{\sqrt{k!}} |k\rangle. \tag{A3}$$

The overlap of the time-evolved state with its initial state is

$$\langle \alpha(0)|\alpha(t)\rangle = e^{-|\alpha|^2} \sum_{k=0}^{\infty} e^{-i\omega k t} \frac{|\alpha|^{2k}}{k!} = \Phi^*(\omega t) \tag{A4}$$

with the characteristic function (discrete Fourier transformation) of the Poisson distribution $P_\nu(k)$ ($\nu = |\alpha|^2$)

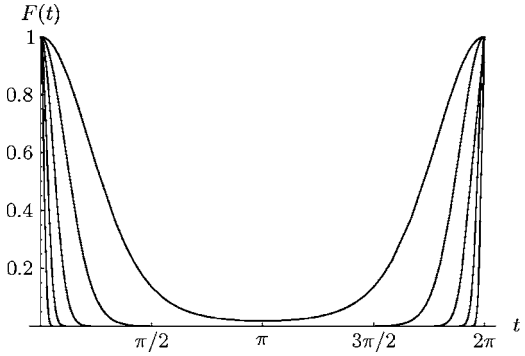

FIG. 19. Fidelity $F(t)$ of Eq. (A7) for $\omega=1$ and α from the set $\{1,2,4,8,16\}$. The larger α is, the smaller is the decay time. t is in units C_C^{-1}.

$$\Phi(t) = \sum_{k=0}^{\infty} e^{ikt} P_\nu(k), \tag{A5}$$

$$\Phi(\omega t) = e^{\nu(e^{i\omega t}-1)} = e^{|\alpha|^2(e^{i\omega t}-1)}. \tag{A6}$$

The fidelity between the two states is then

$$F(t) = |\Phi(\omega t)|^2 = e^{2|\alpha|^2[\cos(\omega t)-1]}. \tag{A7}$$

F is periodic with the oscillator frequency (see Fig. 19). The characteristic time t_c for the decay of F from 1 to $1/e$ is

$$t_c = \frac{1}{\omega}\arccos\left(1 - \frac{1}{2|\alpha|^2}\right). \tag{A8}$$

With the approximation

$$\arccos(1-y) \approx \sqrt{2y}, \quad y \ll 1 \tag{A9}$$

we get

$$t \approx \frac{1}{\omega|\alpha|} \equiv \frac{1}{\omega\sigma} \tag{A10}$$

with σ the standard deviation of the Poisson distribution. Thus the broader the state distribution, the smaller is the time for $F(t)$ to drop to a negligible value.

2. Overlap between uniformly superimposed states

Taking now as the initial state a uniform distribution in the amplitudes (occupation numbers) over all the possible states (n is the cutoff),

$$|\psi(0)\rangle = \frac{1}{\sqrt{n}}\sum_{k=0}^{n-1} |k\rangle, \tag{A11}$$

we get [cf. Eq. (26)]

$$F(t) = |\langle\psi(0)|\psi(t)\rangle|^2 = \left|\frac{1}{n}\sum_{k=0}^{n-1} e^{-i\omega kt}\right|^2 \tag{A12}$$

$$= \frac{\cos(n\omega t)-1}{n^2[\cos(\omega t)-1]}. \tag{A13}$$

This function is not as smoothly decreasing as $F(t)$ of the last section but has zero points, the first one at

$$t_c = \frac{\pi}{2n\omega}, \tag{A14}$$

so again, as n is a measure of the width of the state distribution, the broader the distribution is, the smaller is the dropping time.

[This can be seen as a finite version of the Fourier pair $\delta(t) \leftrightarrow 1$ in the case $n \to \infty$.]

3. Overlap between a normally and a uniformly superimposed state

There are no analytical results available for the overlap between coherent and uniformly superimposed states because of the square root involved in the definition of the coherent state. But for large excitations $|\alpha|$ the state can be described approximately as a state with a normal distribution in both the amplitudes and the occupation numbers.

For the initial state

$$|\psi(t=0)\rangle = \frac{c}{(2\pi)^{1/4}\sqrt{\sigma}}\sum_{k=0}^{\infty} e^{-(k-\mu)^2/4\sigma^2}|k\rangle \tag{A15}$$

and the uniformly distributed state

$$|\psi_{\text{uniform}}\rangle = \frac{1}{\sqrt{n}}\sum_{k=0}^{n-1} |k\rangle \tag{A16}$$

($\mu \gg 1$, c is for adjusting the normalization, $n \gg \mu$), the unitary time evolution (for $\omega=1$ for simplicity)

$$\hat{U}(t) = \sum_{k=0}^{\infty} e^{-ikt}|k\rangle\langle k| \tag{A17}$$

leads to the fidelity

$$F(t) = |\langle\psi_{\text{uniform}}|\hat{U}(t)|\psi(0)\rangle|^2 = \left|\frac{c}{\sqrt{n}(2\pi)^{1/4}\sqrt{\sigma}}\sum_{k=0}^{n-1} e^{-(k-\mu)^2/4\sigma^2}e^{-ikt}\right|^2. \tag{A18}$$

Neglecting the periodicity in time, we can evaluate this discrete form in the continuum limit. As the Fourier transform of a Gaussian is a Gaussian again, we get

$$F(t) = \frac{c^2}{n}\frac{\sqrt{2\pi}}{\tilde{\sigma}}e^{-t^2/2\tilde{\sigma}^2}, \quad \tilde{\sigma} = \frac{1}{2\sigma} \tag{A19}$$

and finally

$$t_c = \frac{1}{2\sigma}. \tag{A20}$$

Again, $F(t)$ drops to $1/e$ of its maximum value in a time antiproportional to the width σ of the distribution over the

states in the oscillator. Note that it drops even faster than the fidelity for coherent states. The maximum amplitude can be set arbitrarily (also to 1) by using non-normalized uniform distributed states.

APPENDIX B: CONSTRUCTING A PURE COHERENT STATE WITH THE SAME FIRST OFF-DIAGONAL DENSITY-MATRIX ELEMENTS AS OF A GIVEN MIXED STATE

Given a mixed state $\hat{\tilde{\rho}}$ containing not only "coherent energy" but "incoherent energy" too, one may ask whether it is possible to split the state into one state $\hat{\rho}=|\psi\rangle\langle\psi|$ containing all the coherent energy and one state $\hat{r}$ containing incoherent energy only. While one can construct a pure state $\hat{\rho}$ that has the same first off-diagonal as $\hat{\tilde{\rho}}$, a state decomposition of $\hat{\tilde{\rho}}$ into this $\hat{\rho}$ and the rest is, in general, not possible.

In order to show this, let

$$|\psi\rangle = \sum_{k=1}^{n} a_k |k\rangle \tag{B1}$$

be a pure state in Fock space representation. The corresponding density-matrix elements are thus

$$\rho_{kl} = a_k a_l^* \tag{B2}$$

and their absolute values

$$|\rho_{kl}|^2 = |a_k|^2 |a_l|^2. \tag{B3}$$

We equate the absolute squares of the first off-diagonal of both $\hat{\tilde{\rho}}$ and $\hat{\rho}$. (Note that the phase in $\tilde{\rho}_{k,k+1}$ can be trivially set by a phase difference between a_k and a_{k+1}^*.) Thus the modulus square of the first off-diagonal

$$f_k = |\tilde{\rho}_{k,k+1}|^2 =: |\rho_{k,k+1}|^2 = |a_k|^2 |a_{k+1}|^2 \tag{B4}$$

can be written with $b_k=|a_k|^2$ in the form of $n-1$ equations

$$b_k b_{k+1} = f_k \tag{B5}$$

with the normalizing condition

$$\sum_k b_k = 1. \tag{B6}$$

If we set $b_1=x$ with fixed x, this would result in

$$q_1 = b_1 = x,$$

$$b_1 b_2 = f_1, \quad c_1 = b_2 = \frac{f_1}{b_1} = \frac{f_1}{x},$$

$$b_2 b_3 = f_2, \quad q_2 = b_3 = \frac{f_2}{b_2} = \frac{f_2}{f_1} x,$$

$$b_3 b_4 = f_3, \quad c_2 = b_4 = \frac{f_3}{b_3} = \frac{f_1 f_3}{f_2 x},$$

$$b_4 b_5 = f_4, \quad q_3 = b_5 = \frac{f_4}{b_4} = \frac{f_2 f_4}{f_1 f_3} x,$$

$$\cdots \tag{B7}$$

as we can recursively define

$$b_{k+1} = \frac{f_k}{b_k}. \tag{B8}$$

With the help of

$$q_k = b_{2k-1}, \quad c_k = b_{2k}, \quad k = 1 \cdots \begin{cases} \frac{n}{2}, & n \text{ even} \\ \frac{n-1}{2}, & n \text{ odd} \end{cases} \tag{B9}$$

we can write Eq. (B6) as

$$x \sum_l q_l + \frac{1}{x} \sum_k c_k = 1 \tag{B10}$$

or as the quadratic equation

$$x^2 \sum_l q_l - x + \sum_k c_k = 0 \tag{B11}$$

with the two solutions

$$x_{1/2} = \frac{1 \pm \sqrt{1 - 4 \sum_l q_l \sum_k c_k}}{2 \sum_l q_l}. \tag{B12}$$

As a scaling of f_k by m

$$f_k' = m f_k \tag{B13}$$

results in a different scaling in the c_k and q_k,

$$c_k' = c_k, \quad q_k' = m q_k, \tag{B14}$$

we can always choose a certain m to fulfill

$$4 \sum_l q_l \sum_k c_k = 1 \tag{B15}$$

and therefore get from Eq. (B12) a single solution. Note that the scaling factor m needed to account for possible decoherence in the data drops out of this calculation automatically.

If we numerically test

$$\hat{r} = \hat{\tilde{\rho}} - \frac{1}{\sqrt{m}} |\psi\rangle\langle\psi| \tag{B16}$$

for our system, we find that $\hat{r}$ is no longer positive (for times $t \neq 0$) and thus no longer a density operator. The first off-diagonal coherence can therefore not be accounted for by a single pure state.

The eigenstates do show typically components in the first off-diagonal, underlining the impossibility to decompose this part into a single pure state.

APPENDIX C: INVARIANCE OF THE OSCILLATOR STATE UNDER THE INFLUENCE OF THE ENVIRONMENT IN THE CLASSICAL LIMIT

According to Eqs. (22) and (23), $\hat{\rho}$ was subject to coherent evolution only, if

$$\hat{L}_{\mathrm{inc}}\hat{\rho} = 0. \tag{C1}$$

As the subsystems C and G are separable in the classical limit and condition (C1) certainly does not hold for the system G (as required), we only regard system C. Note that even if the oscillator C remains coherent and is invariant under bath action, it nevertheless can act via operators of the form $\sigma_{\pm} \otimes \hat{\Pi}$ on the system G. We will see that the action applied to the quantum system G is then a classical parametric control.

The corresponding environment operator $\hat{A}$ acting on the system C is in its simplest case (no cutoff procedure being involved and thus hermiticity preserved) of the form

$$\hat{A} = \hat{A}^{\dagger} = \hat{\Pi} \tag{C2}$$

with the matrix representation in Fock basis

$$\Pi_{kl} = \frac{1}{2\pi}\int_{\tau \in \Theta_{\omega}} \theta(\tau) e^{-i(k-l)\tau} d\tau = \Pi_{(k-l)}, \tag{C3}$$

where $\Theta_{\omega=1} = [-\pi, \pi]$ (the oscillator frequency ω is set to 1, for simplicity).

If for the initial state $\hat{\rho}_{\mathrm{C}} = |\alpha\rangle\langle\alpha|$

$$\hat{\Pi}|\alpha\rangle = c|\alpha\rangle, \tag{C4}$$

it would follow that, indeed,

$$\hat{L}_{\mathrm{inc}}\hat{\rho}_{\mathrm{C}} = \hat{\Pi}|\alpha\rangle\langle\alpha|\hat{\Pi} - \frac{1}{2}\hat{\Pi}\hat{\Pi}|\alpha\rangle\langle\alpha| - \frac{1}{2}|\alpha\rangle\langle\alpha|\hat{\Pi}\hat{\Pi} = 0. \tag{C5}$$

The eigenvalue c can even be a function of time, as $|\alpha\rangle = |\alpha(t)\rangle$ might be considered as a unitarily evolving oscillator state.

In the following we will show that Eq. (C4) holds for $|\alpha| \to \infty$ with eigenvalue $c = \theta(t)$, i.e.,

$$\langle\alpha|\hat{\Pi}|\alpha\rangle = c \quad \text{for} |\alpha| \to \infty. \tag{C6}$$

Instead of considering a time-dependent state with a complex phase and a fixed control function $\theta(\tau)$, we consider a fixed state with phase zero and a cyclically time-shifted $\theta(\tau)$ (in the interval Θ_{ω}) to examine the invariance properties at an arbitrary time (only the relative phase and thus relative time matters).

With the Fock representation $|l\rangle$ of the Gaussian approximated square root of Poisson distributions ($\mu = \nu, \sigma^2 = \nu, \nu = |\alpha|^2, \alpha \in \mathbb{R}_+$, good for $\nu \gg 1$)

$$\sum_l |l\rangle\langle l| = 1, \quad \langle l|\alpha\rangle \equiv \psi_l = \frac{e^{-(l-\nu)^2/4\nu}}{(2\pi\nu)^{1/4}}, \tag{C7}$$

the eigenvalue equation in this representation and the overlap between $\langle\alpha|$ and $\hat{\Pi}|\alpha\rangle$, respectively, read

$$\langle k|\hat{\Pi}|\alpha\rangle = \sum_l \Pi_{kl}\psi_l = c\psi_k, \tag{C8}$$

$$c = \langle\alpha|\hat{\Pi}|\alpha\rangle = \sum_k \sum_l \psi_k^* \Pi_{kl} \psi_l, \quad k,l \in \mathbb{N}_0^+. \tag{C9}$$

The discrete nature of the last equation stems from the periodicity of the harmonic-oscillator time evolution. It is convenient to evaluate the overlap with the help of continuous functions and not in the half-space but rather in full space, which is a good approximation near the classical limit [$\theta(\tau)$ can be set to zero outside of Θ_{ω} for the discussion in the continuum limit]. Then we have to evaluate

$$c = \int_{-\infty}^{\infty}\int_{-\infty}^{\infty} f(k)p(k-l)f(k)dk\,dl \tag{C10}$$

with $f(k) = \psi_k$, $p(k-l) = \Pi_{kl}$, and $k, l \in \mathbb{R}$ (note that Π_{kl} is only a function of $k-l$, and that $\psi_k = \psi_k^*$).

In the continuum limit, Eq. (C8) reads

$$\int_{-\infty}^{\infty} p(k-l)f(l)dl = cf(k). \tag{C11}$$

A special solution is $f(l) = \text{const}$. This would be an allowed eigenfunction of $\hat{\Pi}$.

With the variable transformation

$$l \to l - \nu, \tag{C12}$$

$$k \to k - \nu, \tag{C13}$$

the function f is even,

$$f(l) = \frac{e^{-l^2/4\nu}}{(2\pi\nu)^{1/4}}, \tag{C14}$$

while leaving $p(k-l)$ and thus the overlap in Eq. (C10) invariant. Approaching the classical limit $f(l)$ becomes broader; finally the width $\sqrt{2\nu}$ goes to infinity and $f(l)$ virtually becomes a constant, i.e., an eigenfunction of $\hat{\Pi}$. [The complex exponentials $e^{st}, s \in \mathbb{C}$ are eigenfunctions for all linear time-invariant systems, so the constant function 1 (for $s = 0$) and likewise $|\alpha\rangle$ in the classical limit is an eigenfunction of $\hat{\Pi}$.] This proves Eq. (C4).

We now turn to the calculation of c according to Eq. (C10). This equation involves a convolution of p with f, so a transformation into Fourier space is useful: We see that the Fourier transforms

$$F(\kappa) = \mathcal{F}_{\kappa}[f(k)] = \int_{-\infty}^{\infty} f(k)e^{i\kappa k}dk, \tag{C15}$$

$$P(\kappa) = \mathcal{F}_\kappa[p(k)] = \int_{-\infty}^{\infty} p(k) e^{i\kappa k} dk \tag{C16}$$

are real functions as $f(k)$ is even and

$$p(k) = \frac{1}{2\pi} \int_{\tau \in \Theta_\omega} \theta(\tau) e^{-ik\tau} d\tau = \mathcal{F}_\tau^{-1}[\theta(\tau)](k). \tag{C17}$$

It thus holds, in agreement with Eq. (C3), that

$$P(\kappa) = \theta(\kappa), \tag{C18}$$

which is real by construction.

Applying the convolution theorem ($\mathcal{F}[f*g] = \mathcal{F}[f]\mathcal{F}[g]$) twice and using the symmetry of $f(k)$, we get

$$\begin{aligned} c &= \int_{-\infty}^{\infty} \int_{-\infty}^{\infty} f(k) p(k-l) f(l) dk\, dl \\ &= \int_{-\infty}^{\infty} f(k) \mathcal{F}_\kappa^{-1}[P(\kappa)F(\kappa)](k) dk \\ &= \int_{-\infty}^{\infty} f(0-k) \mathcal{F}_\kappa^{-1}[P(\kappa)F(\kappa)](k) dk \\ &= \mathcal{F}_k^{-1}[F(\kappa)P(\kappa)F(\kappa)](0) \\ &= \frac{1}{2\pi} \int_{-\infty}^{\infty} P(\kappa) F^2(\kappa) d\kappa. \end{aligned} \tag{C19}$$

For the calculation of $F(\kappa)$ according to Eq. (C15), we observe that the Fourier transform of a Gaussian is a Gaussian and thus also $F^2(\kappa)$. We thus find

$$F^2(\kappa) = \frac{\sqrt{2\pi}}{\tilde{\sigma}} e^{-\kappa^2/2\tilde{\sigma}^2}, \quad \tilde{\sigma} = \frac{1}{2\sqrt{\nu}}. \tag{C20}$$

In the classical limit, we get

$$\lim_{\nu = |\alpha|^2 \to \infty} F^2(\kappa) = 2\pi\delta(\kappa). \tag{C21}$$

Plugging this into Eq. (C19) and obeying Eqs. (C9), (C10), and (C18) we see that

$$\lim_{|\alpha|^2 \to \infty} c = \lim_{|\alpha|^2 \to \infty} \langle \alpha | \hat{\Pi} | \alpha \rangle = \theta(0). \tag{C22}$$

We thus have shown that for $|\alpha| \to \infty$,

$$\Pi |\alpha(t)\rangle = \theta(t) |\alpha(t)\rangle \quad (t \text{ cyclic in } \Theta_\omega), \tag{C23}$$

where $\theta(t)$ is the Fourier transform of $\Pi_{(k-l)}$, the Fock representation of $\hat{\Pi}$. This arbitrary control function is a constant at any fixed time. If we shift the function $\theta(t)$ in the interval Θ_ω cyclically, we get the same overlap as for a time-dependent oscillator state. Thus, the control function $c = \theta(t)$ controls in the classical limit exactly the system G in a parametric fashion.

[1] B. Diu, C. Guthmann, D. Lederer, and B. Roulet, *Éléments de Physique Statistique* (Hermann Editions des Sciences et des Arts, Paris, 1989).

[2] J. Gemmer, M. Michel, and G. Mahler, *Quantum Thermodynamics: Emergence of Thermodynamic Behavior Within Composite Quantum Systems*, Vol. 657 of Lecture Notes in Physics (Springer, Berlin, 2004).

[3] P. Borowski, J. Gemmer, and G. Mahler, Eur. Phys. J. B **35**, 255 (2003).

[4] G. Lindblad, Commun. Math. Phys. **48**, 119 (1976).

[5] U. Weiss, *Quantum Dissipative Systems*, 2nd ed. (World Scientific, Singapore, 1999).

[6] M. Michel, M. Hartmann, J. Gemmer, and G. Mahler, Eur. Phys. J. B **34**, 325 (2003).

[7] T. Feldmann and R. Kosloff, Phys. Rev. E **68**, 016101 (2003).

[8] R. Kosloff and T. Feldmann, Phys. Rev. E **65**, 055102(R) (2002).

[9] E. Geva and R. Kosloff, J. Chem. Phys. **97**, 4398 (1992).

[10] J. P. Palao, R. Kosloff, and J. M. Gordon, Phys. Rev. E **64**, 056130 (2001).

[11] M. O. Scully, Phys. Rev. Lett. **87**, 220601 (2001).

[12] M. O. Scully, Phys. Rev. Lett. **88**, 050602 (2002).

[13] C. M. Bender, D. C. Brody, and B. K. Meister, Proc. R. Soc. London, Ser. A **458**, 1519 (2002).

[14] B. Lin and J. Chen, Phys. Rev. E **67**, 046105 (2003).

[15] A. E. Allahverdyan, R. Balian, and T. Nieuwenhuizen, e-print cond-mat/0402387.

[16] T. D. Kieu, Phys. Rev. Lett. **93**, 140403 (2004).

[17] T. E. Humphrey, R. Newbury, R. P. Taylor, and H. Linke, Phys. Rev. Lett. **89**, 116801 (2002).

[18] J. M. R. Parrondo and B. J. D. Cisneros, Appl. Phys. A **75**, 179 (2002).

[19] F. C. Lombardo and P. I. Villar, Phys. Lett. A **336**, 16 (2005).

[20] L. E. Ballentine, *Quantum Mechanics*, 2nd ed. (World Scientific, Singapore, 1998).

[21] R. Alicki and M. Fannes, *Quantum Dynamical Systems* (Oxford University Press, Oxford, 2001).

[22] M. A. Nielsen and I. L. Chuang, *Quantum Computation and Quantum Information* (Cambridge University Press, Cambridge, U.K., 2000).

[23] R. B. Sidje, ACM Trans. Math. Softw. **24**, 130 (1998).

[24] C. Ashcraft and R. Grimes, SPOOLES—An Object Oriented Software Library for Solving Sparse Linear Systems of Equations (1999), www.netlib.org/linalg/spooles/.

[25] R. B. Lehoucq, D. C. Sorensen, and C. Yang, ARPACK Users' Guide: Solution of Large-Scale Eigenvalue Problems by Implicitly Restarted Arnoldi Methods (SIAM, Philadelphia, 1998).

[26] F. L. Curzon and B. Ahlborn, Am. J. Phys. **43**, 22 (1975).

[27] S. D. Franceschi and L. Kouwenhoven, Nature (London) **417**, 701 (2002).

[28] *Handbook of Nanoscience, Engineering and Technology*, edited by W. A. Goddard III, D. Brenner, S. E. Lyshevski, and G. J. Iafrate (CRC, Boca Raton, FL, 2002); M. Paulsson, F. Zahid, and S. Datta, *Resistance of a Molecule*, Vol. 27 of Electrical Engineering Textbook Series, see also cond-mat/0208183.